Sensors & Actuators: B. Chemical 380 (2023) 133273

Contents lists available at ScienceDirect

Sensors and Actuators: B. Chemical

journal homepage: www.elsevier.com/locate/snb

A novel comparative study for simultaneous determination of Cd (II) and Pb (II) based on ruthenium complex-nanoparticles-nafion modified screen-printed gold electrode

Ibtihaj Albalawi, Anna Hogan, Hanan Alatawi, Samia Alsefri, Eric Moore *

Sensing and Separation Group, School of Chemistry,University College Cork, Cork, Ireland

ARTICLE INFO

Keywords:
Heavy metal ions
Ruthenium (II) bipyridine
Graphene oxide
Gold-citrated
Nafion
Screen printed electrode

ABSTRACT

A novel and effective method for immobilization of active ruthenium (II) bipyridine complex on screen printed gold electrode surface was developed for simultaneous determination of Cd (II) and Pb (II) in an environmental water sample. The electrostatic interaction between negatively charged graphene oxide (GO) or citrate-capped gold nanoparticles (AuNPs) and positively charged ruthenium (II) bipyridine complex ($[Ru(bpy)_3]^{2+}$) was studied with the incorporation of cation exchanging Nafion polymer, which enhanced electron transfer rate, reduced the interference caused by active compounds and results in long term stability. The comparison between the hybrid Ru-GO/Nafion and Ru-Au/Nafion nanocomposites' behavior was electrochemically investigated in this paper through cyclic voltammetry (CV), electrochemical impedance spectroscopy (EIS), and square wave anodic stripping voltammetry (SWASV). Additionally, the surface morphologies of the screen-printed electrode were evaluated using energy-dispersive X-ray spectroscopy (EDX) and scanning electron microscopy (SEM). The proposed Ru-GO/Nafion sensor exhibited a higher sensitivity towards cadmium ion with a detection limit of 4.2 ppb compared to the Ru-Au/Nafion assay, which reveals low sensitivity with a limit of detection of 12.01 ppb. The developed assays show excellent electrochemical performance towards lead ions with a detection limit of 5.3 ppb and 2.5 ppb for Ru-GO/Nafion and Ru-Au/Nafion, respectively, indicating that the lead ions can be accumulated more on the surface of Ru-Au/Nafion SPGE. The hybrid nanocomposite assays were successfully employed in river and tap water samples and validated using Atomic Absorption Spectroscopy (AAS).

1. Introduction

Heavy metals are particularly damaging contaminants in the biosphere, and even trace concentrations represent a risk to human health due to their toxicity [1]. Thus, it is critical to develop an analytical approach that is simple, fast, and sensitive for the determination and monitoring of these toxic contaminants in the aquatic environment. There are numerous conventional techniques for analyzing heavy metals, including atomic absorption spectroscopy [2,3], inductively coupled plasma emission spectrometry [4,5], and inductively coupled plasma mass spectrometry [6,7]. These spectrometric approaches, however, are extremely expensive and unsuitable for in situ monitoring due to the instrumentation's bulk and complexity. On the other hand, electrochemical strategies have been introduced as an effective method for metal ions detection as an alternative to these spectroscopic techniques due to their portability, short processing time, high sensitivity, and low cost [8]. Among several electrochemical procedures, electrochemical stripping voltammetric analysis is a particularly effective approach for metal ions determination because it is highly sensitive and capable of simultaneously analyzing numerous heavy metal ions [9,10].

The chemical modifiers are extensively used to enhance the efficiency of accumulation ions and increase the sensitivity of the stripping method [11]. Various nanomaterials are generally employed for heavy metal ions detection [12]. Among them are carbon-based nanomaterials, which have recently gained significant attention from researchers due to their distinctive features and potential for applications in various nanotechnology-related fields.[13]. Graphene and graphene oxide are such types of carbon-based nanostructures, which are readily used in a wide range of applications due to their distinct physical and chemical properties such as high potential adsorption capacity, large specific surface area, superior electrical and thermal conductivity [14]. Rather

* Corresponding author.
E-mail address: e.moore@ucc.ie (E. Moore).

https://doi.org/10.1016/j.snb.2022.133273
Received 18 October 2022; Received in revised form 18 December 2022; Accepted 28 December 2022
Available online 5 January 2023

than using graphene alone, scientists have employed the graphene oxide (GO) form, which has excellent oxidant characteristics in addition to the existence of carboxyl (eCOOH), hydroxyl (eOH), and epoxy (CeOeC) functional groups, which make it more appropriate for processing, synthesizing, application and more easily spread. [15] Compared to graphene, GO has proved to be a superior material for a variety of applications, including the purification of drinking water due to its imperishable hydrophilicity. Additionally, GO exhibits excellent π - π conjunction and doping properties for inorganic or organic complexes, such as ruthenium (II) complexes based on the pyrene moiety [16]. This complex has the potential to further increase the efficiency of mass transport and charge transfer as well as sensitivity and selectivity due to their unique properties, including excellent chemical stability, strong visible light harvesting property, photophysical, photochemical, and redox properties that are highly applicable at both the ground and excited states, as well as electron-transfer processes and versatile excited-state energy [17].

Metal-based nanomaterials have also presented distinct advantages in numerous areas, and they are currently an exciting area of research since they allow for a new level of freedom in varying the particle properties by combining two metals in a single particle. This broadens their potential used in electrocatalysis [18]. Gold nanoparticles are among the most common and promising conducting nanomaterials due to their fascinating optical and electrical properties, in addition to their unique stability [19]. It has recently received considerable attention due to its ease of synthesis as well as its unique environmental and biomedical applications [20]. Generally, many synthetic strategies have been developed to prepare GNPs, including in situ synthesis using reducing agents such as formaldehyde, polyols, oxalic acids, hydrogen peroxide, and sugars [21,22]. It is reported that gold nanoparticles can be generated by the reduction of chloroauric acid using sodium citrate according to the well-known Turkevich method [23], presenting high stability and excellent homogeneity [24]. Also, ruthenium (II) complexes and gold nanoparticles could be electrostatically immobilized on the electrode surface to form (Ru–AuNPs) composites, promising outstanding physical and chemical properties [25,26].

Nafion (NA) is a cation exchange membrane, which is well known for its electrochemical performance and thermal stability [27]. The incorporation of $[Ru(bpy)_3]^{2+}$ into Nafion films can be easily fabricated. However, poor long-term stability of metal complex-based Nafion is the main drawback because the immobilized $[Ru(bpy)_3]^{2+}$ tends to be migrated into the hydrophobic inactive electro area with time [28]. Consequently, the immobilization of $[Ru(bpy)_3]^{2+}$ on the electrode surface has received considerable attention in recent years, and novel methods and materials are being developed to improve long-term stability and sensitivity. Therefore, Various materials have been combined to $[Ru(bpy)_3]^{2+}$–Nafion film to enhance its performance [29,30].

Several ruthenium complexes with immunosensor and DNA probe assays have been reported in medical applications [31–33]. However, it is rather unfortunate that less attention is being given to ruthenium-based sensors for heavy metal detection, and few papers have been reported. In terms of environmental analysis, in 2017, the dip coating technique was employed to deposit a thin film of Nafion doped with $[Ru(bpy)_3]^{2+}$ on ITO-coated glass substrates to detect cadmium and lead using anodic stripping voltammetry [34]. In an earlier report in 2017, Gump et al. demonstrated for the first time $[Ru(bpy)_3]^{2+}$-GO nanocomposite for simultaneous detection of heavy metal ions in water [35]. The active redox molecule (ruthenium (II) complex) is integrated on the surface of GO to improve the inherent electrical conductivity. In this research, $[Ru(bpy)_3]^{2+}$ was incorporated into the graphene oxide through the electrostatic and π-π stacking interactions for simultaneous detection of cadmium and lead in water samples. Also, the cation-exchange Nafion polymer was incorporated into the GO–Ru hybrid materials, which has a major contribution to accelerating electron transport and improving stability. For comparison, gold nanoparticles electrostatically incorporated to $[Ru(bpy)_3]^{2+}$ and dispersed in Nafion polymer. Additionally, the screen-printed electrode was selected due to its electro response which provides great surface area for electrostatic π-π interactions for $[Ru(bpy)_3]^{2+}$ ligand binding, and its advantages of great reproducibility, good electrical resistivity, and low cost. Besides, it has the potential to be used as an on-site monitoring system.

2. Experimental

2.1. Materials

Nafion (5 wt % in a mixture of 45 % lower aliphatic alcohols and water), acetic acid, sodium citrate, sodium acetate, sulfuric acid, ethanol, lead (II) nitrate, cadmium (II) nitrate, gold (III) chloride trihydrate, tris(2,2′-bipyridyl) ruthenium (II) dichloride hexahydrate, potassium ferricyanide (III), potassium chloride, and potassium hexacyanoferrate (II) trihydrate were purchased from Sigma Co., Ltd. (Ireland). Deionized water was obtained from the laboratory water system of an ERI (Environmental Research Institution). All ingredients were used exactly as they were received, and all experiments were carried out at room temperature. Disposable screen-printed gold electrode (SPGE)- (refs. 220AT) was purchased from DropSens (Spain). It was fabricated with high temperature curing inks and contains a silver reference electrode. The size of the whole SPGE was 3.4 × 1.0 × 0.05 cm (Length x Width x Height).) and the diameter of the gold working electrode was 4 mm.

2.2. Solutions preparation

Deionized water was used to prepare all the aqueous solutions. Nafion (5 %) was dissolved in anhydrous ethanol to prepare various Nafion concentrations. A stock solution of gold (III) chloride trihydrate (0.1 %) was prepared by dissolving 0.1 g in 100 mL of water and preserved at 4 C. Tris(2,2′-bipyridyl) ruthenium (II) dichloride stock solution was made by dissolving a proper quantity in deionized water. 1 % sodium citrate was prepared by dissolving 0.5 g in 50 mL of water. A 1000 ppm stock solution of Cd (II) and Pb (II) was prepared in an aqueous solution. To make an acidic solution buffer, an adequate amount of sodium acetate was dissolved in 0.1 M acetic acid to adjust the pH to 5.

2.3. $[Ru(bpy)_3]^{2+}$- GO/NA nanocomposite synthesis

Under the dark condition, 5 mL aqueous solution of graphene oxide (2 mg/mL) and 5 mL ethanolic solution of tris(2,2′-bipyridyl) ruthenium (II) dichloride (1 mg/mL) were mixed and stirred at 800 rpm for 12 h. Then, the nanocomposite solution was centrifuged for 40 min at 12,000 rpm and properly cleaned with deionized water and ethanol to remove untreated $[Ru(bpy)_3]^{2+}$ from the suspension. The resulting precipitate was suspended in 1 % ethanolic Nafion solution and sonicated for 30 min.

2.4. $[Ru(bpy)_3]^{2+}$ - AuNPs/NA nanocomposite synthesis

Gold nanoparticles (AuNPs) were prepared by citrate reduction of gold (III) chloride in an aqueous solution. In short, 0.01 g of gold (III) chloride trihydrate was dissolved in 100 mL of water. Then, 3 mL of 1 % sodium citrate solution was added under stirring. After that, the solution was maintained boiling for another 30 min before cooling to room temperature. Prior preparation of Ru-AuNPs, an aqueous solution of 0.05 M tris(2,2′-bipyridyl) ruthenium (II) dichloride was prepared, and 300 μL was taken and added to 20 mL of the previous solution under stirring. A few minutes later, a significant proportion of black precipitate was created [36]. The formed result was centrifuged, rinsed multiple times with water, suspended in 1 % ethanolic Nafion solution, and sonicated for 30 min.

2.5. Physical and electrochemical measurements

The morphological characteristic of modified nanocomposite screen printed electrodes was studied using Scanning Electron Microscopy (SEM); structural studies were carried out using energy dispersive X-ray spectroscopy (EDX). PalmSens (Netherlands) handheld potentiostat/ galvanostat was used to investigate the performance of the electrochemical analysis. cyclic voltammetry (CV) was performed to characterize the electrode surface. For quantitative analysis, square wave anodic stripping voltammetry (SWASV) was carried out for the simultaneous detection of metal ions. A magmatic stirrer was used after impressing the electrodes in a solution of acetate buffer (pH 5.0). The following parameters were performed: frequency; 25 Hz pulse amplitude;50 mV; deposition potential; −1.6 V; deposition time; 120 s

2.6. Fabrication of modified hybrid nanocomposites

Prior to fabrication, screen-printed gold electrodes were electrochemically activated using cyclic voltammetry within the range of 0–1.6 in 0.5 M sulphuric acid at 0.1 V/s scan rate and then cleaned with water and dried at air [37]. Subsequently, 6 μL of Ru-GO/NA and Ru-Au/NA were dropped cast at the SPGE surface and allowed to dry in air. The electrodes were then utilized for electrochemical analysis.

2.7. Real sample preparation

River water samples were collected from River Lee (Cork, Ireland). Prior to sample testing, a 0.22-m filter was used to remove any suspended material. Tap water was obtained from environmental research institution (ERI).

3. Results and discussion

3.1. Characterization of hybrid $[Ru(bpy)_3]^{2+}$ - GO /NA and $[Ru(bpy)_3]^{2+}$- AuNPs /NA nanocomposites

3.1.1. Surface morphology of SPGEs

Scanning electron microscopy (SEM) was employed to examine the surface morphology of GO and Ru-GO/NA nanocomposite. The wrinkled layered structure of graphene oxide can be seen in Fig. 1**.b**, providing ultrathin and homogeneous graphene film. Additionally, The EDX technique was performed to study the chemical elements of nanocomposites. The carbon and oxygen peaks correspond to GO, whereas the signal of florid is attributed to Nafion, as seen in Fig. 1**c.** In comparison to GO, nanocomposite of Ru-GO/NA presented a thick-packed sheet structure with a gently corrugated form (Fig. 1**.d)** [38,39]. Further, the EDX spectra of nanocomposite of Ru-GO/NA is displayed in Fig. 1**.e.**, it revealed an additional peak of ruthenium, indicating that the GO and $[Ru(bpy)_3]^{2+}$ were successfully immobilized on the surface of the screen-printed electrode. The obtained morphology of the synthesized gold nanoparticles is observed in Fig. 1**.f,** which shows uniform polydispersed distribution on the surface with traces of agglomeration [40]. An organic element layer was formed after the Ru-Au coating, and the EDX analysis of the nanocomposite revealed the presence of the Ru element (Fig. 1**.i**) [41,42]. Further confirmation through the use of energy-dispersive X-ray spectroscopy measurement reveals the presence of Ru, Au, N, O, and C elements, demonstrating that the Ru complex was modified on the electrode surface [42].

3.1.2. Electrochemical characterisation of hybrid $[Ru(bpy)_3]^{2+}$- GO /NA and $[Ru(bpy)_3]^{2+}$- AuNPs /NA nanocomposites

The electrochemical performance of hybrid nanocomposite modified electrodes was studied using cyclic voltammetry in the presence of 1 mM $K_3[Fe(CN)^6]$ in 0.1 M KCl solution at a scan rate of 0.1 V/s. A well -defined redox peak appears at bare SPGE, and when the electrode surface was modified with Nafion, the Polymeric Nafion film inhibited the one-electron redox behavior of $Fe(CN)^{6\ 3-/4-}$ and the cathodic and anodic peaks were nearly disappeared. The redox couple peaks were observed again due to the existence of graphene oxide in the composite film, which immobilized on the electrode surface, demonstrating that the conductive graphene facilitates electron transfer. Obviously, further increase in redox probe at Ru-GO /NA/ SPGE, demonstrating that the rate of electron transfer had significantly improved as a result of the GO and Ru-GO nano-interface electrocatalytic behavior (Fig. 2**. a)** Also, the conductive AuNPs enhanced the electron surface, and the redox probe shows a significate increase compared to the bare electrode, as seen in Fig. 2**. b.** Dramatic reduction in the redox peak was noticed when the Ru- AuNPs /NA was coated on the surface of SPGE, which is due to the kinetics barrier between $[Fe(CN)^6]^{4-}$/ $[Fe(CN)^6]^{3-}$ and the negatively charged Nafion.

Further confirmation was also found by cyclic voltammograms; the reversibility and diffusion-controlled properties of the redox probe were evaluated for modified Ru-GO/NA and Ru-Au /NA nanocomposite electrodes. The plots of peak currents vs. square roots of scan rate were seen in Fig. 2**. c, d**, indicating that the reversible electron transfer reaction is completely diffusion-controlled as the relationship between peak current and the square root is linear with r values of 0.997 for Ru-GO /NA/ SPGE and 0.996 for Ru-Au /NA/ SPGE.

Electrochemical impedance spectroscopy (EIS) was used to evaluate the nanocomposite modified electrodes' interface properties (Fig. 3**.a**). The equivalent circuit model used to fit the EIS data has also been represented in (Fig. S1 in supporting materials). The line at a low frequency is related to the diffusion-controlled system, and the impedance spectra at a high frequency correspond to the kinetic controlled process. The values of charge transfer resistance (R_{ct}) were determined based on the values of semicircle diameter, which is equivalent to the resistances to faradaic charge transfer. Obviously, the lowest semicircle could be found in the bare EIS plot, indicating a slower electron transfer resistance of the redox probe. After the Nafion film coated the SPE surface, the R_{et} was largely improved as a result of the existence of sulfonic groups in Nafion film, which could inhibit $[Fe(CN)6]^{3-/4-}$ from reaching the electrode surface at low frequencies**.** In contrast, the R_{ct} of the GO/NA/SPGE decreased rapidly (R_{ct} ∼ 1750 Ω) but remained greater than that of bare SPGE, suggesting that the graphene oxide had excellent electrical conductivity and had the potential to accelerate electron transfer. Following the incorporation of the ruthenium complex into the nanocomposite, the charge transfer resistance was reduced (R_{ct} ∼ 750 Ω), indicating superior electrical conductivity of hybrid nanomaterial, which can enhance the electron transfer and mass exchange of electro-active indicators on the surface. The electrochemical response of AuNPs was nearly a straight line, which is a typical property of the diffusion process [43]. Obviously, a significant increase was obtained after coating the surface with Ru-Au/ NA, attributed to the fact that the electron hindered the redox probe towards the surface of the electrode.

The effective electroactive surface area for modified nanocomposite sensors was determined using the Randles-Sevcik equation [44], as shown below:

$$I_{p,f}^{rev} = \pm 0.446 n F A_{rel} C \sqrt{\frac{nFDv}{RT}} \quad (1)$$

Where n is the number of electrons in the electrochemical reaction, $I_{p,f}$ is the voltammetric current using the forward peak of the electrochemical process, F is the Faraday constant (96,485 C/mol), v is the applied voltammetric scan rate (V/s), T is the temperature in Kelvin (273.15), R is the universal gas constant (8.314 J/mol/K), A_{rel} is the electroactive area of the electrode (cm^2) and D is the diffusion coefficient in cm^2/s.

Thus, A_{rel} was calculated to be 0.0763 cm^2 and 0.025 cm^2 for Ru-GO /NA/ SPGE and Ru-Au /NA, respectively. The A_{rel} values were compared to A_{geo} values, and % real were determined to be 95.38 % for Ru-GO /NA/ SPGE and 83.33 % for Ru-Au /NA/SPGE using the following equation:

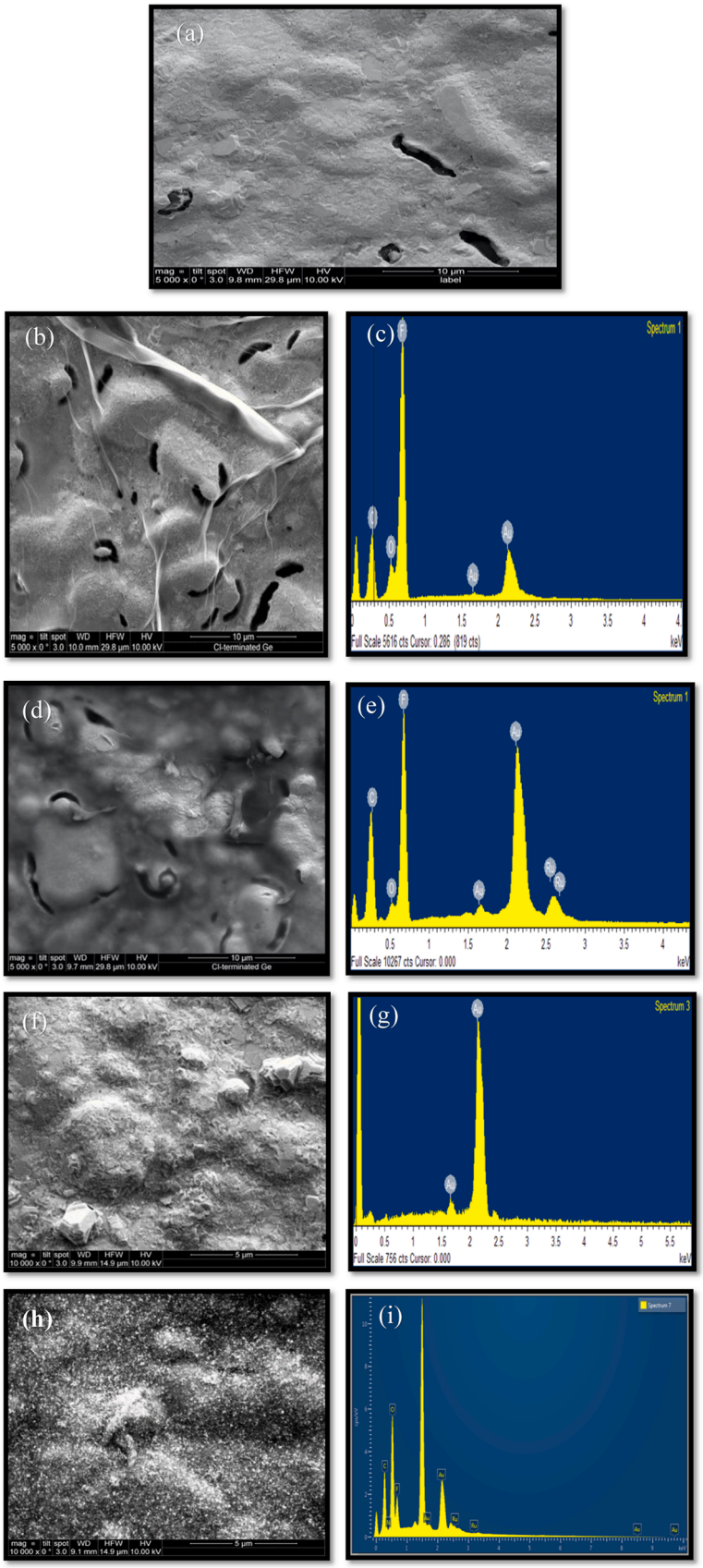

Fig. 1. SEM images of bare (a), GO/NA/SPGE (b), GO-Ru/NA/SPGE (d) at 5000 magnifications: Au-citrated /SPGE (f) and Au-Ru/NA/SPGE (h) at 10000 magnifications. EDX spectrum of GO/NA/SPGE (c), GO-Ru/NA/SPGE (e), Au-citrated /SPGE (g) and Au-Ru/NA/SPGE (i).

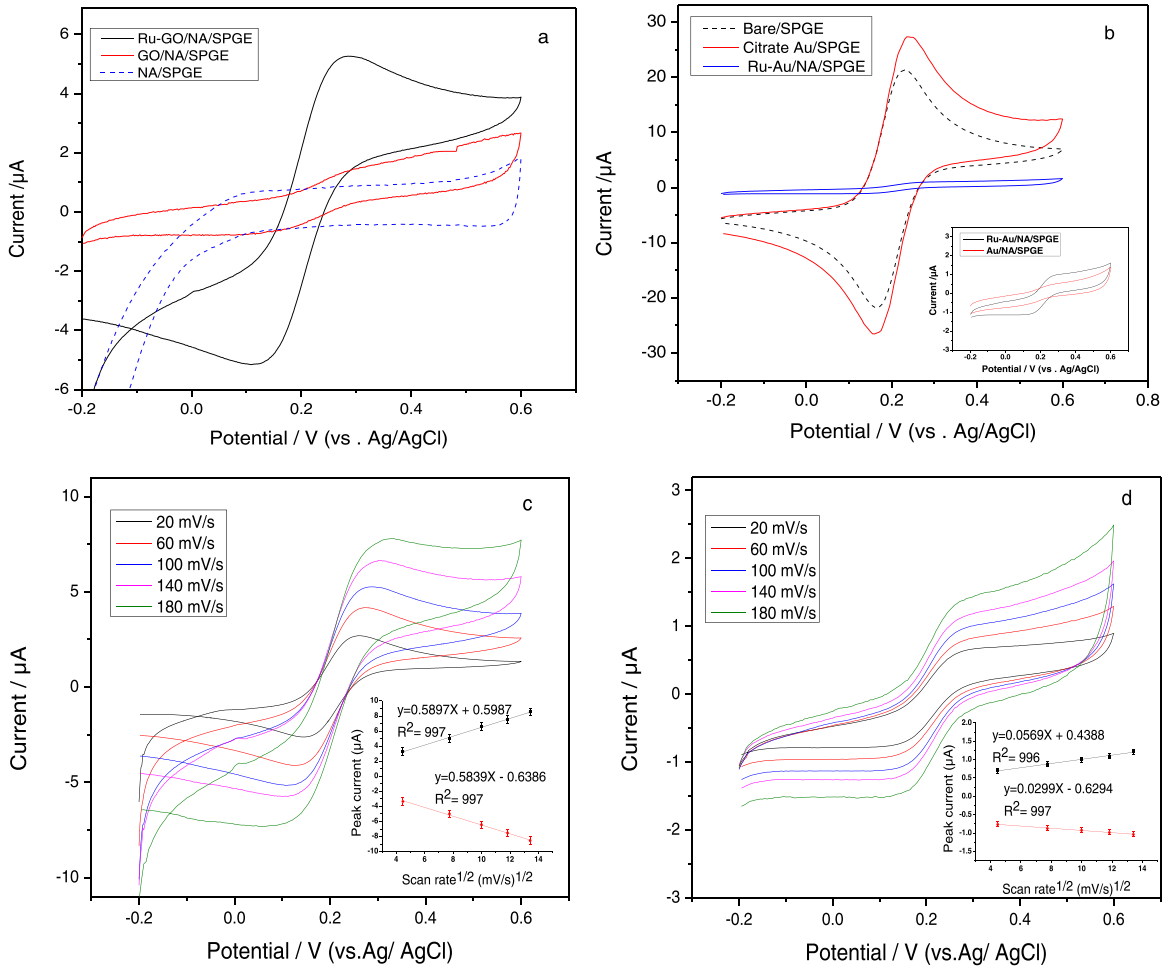

Fig. 2. Cyclic voltammograms of NA/SPGE and GO-NA/SPGE and GO-Ru/NA/SPGE (a), Cyclic voltammograms of bare SPGE, AuNPS/SPGE, Au-Ru/NA/SPGE (b), Au/NA/SPGE and Au-Ru/NA/SPGE (b inset); in 1 mM K_3[Fe (CN)^6] in 0.1 M of KCl. Cyclic voltammograms of GO-Ru/NA/SPGE (c) and Au-Ru/NA/SPGE (d) with various scan rates from 20 to 180 mV/s. Anodic and cathodic peak currents vs. square root of scan rate for GO-Ru/NA/SPGE (c inset) and Au-Ru/NA/SPGE (d inset).

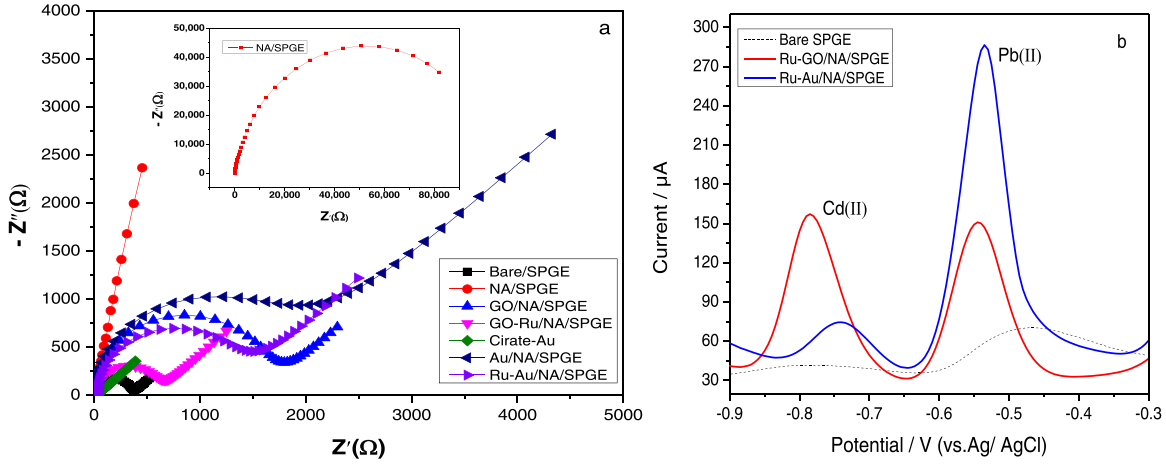

Fig. 3. (a) Nyquist plot of 1 mM K_3[Fe (CN)^6] in 0.1 M of KCl at bare SPCE, NA/SPGE, GO/NA/SPGE, GO-Ru/NA/SPGE, AuNPs/SPGE, Au/NA SPCE and Au-Ru/NA/SPGE. (b) SWASV of 200 ppb Cd (II) and Pb (II) in 0.1 M acetate buffer (pH 5.0) at bare SPCE, GO-Ru/NA/SPGE and Au-Ru/NA/SPGE.

$$\%\text{Real} = (A_{rel}/A_{geo}) \times 100 \quad (2)$$

This assumes that GO interfusion could increase the load quantity of $[Ru(bpy)_3]^{2+}$ in the Nafion film more than the interfusion of AuNPs.

Additionally, electrochemical impedance spectroscopy was used to study the charge transport process of GO-Ru/NA/SPGE and Ru-Au /NA/SPGE. The electron transfer rate constant (K_{et}) values were determined using Eq. (1), as shown below.

$$K_{et} = RT / n^2 F^2 A C_0 R_{ct} \quad (3)$$

Where R is the gas constant (8.314 J/K mol), T is the temperature in

Kelvin degrees, n is the number of electrons, F is Faraday's constant (96,485 C/mol), A is the electrode surface area in cm^2, C is the redox probe concentration in mol/L and R_{ct} is the charge transfer resistance in Ω, which was determined based on impedance measurements. The k_{et} values of Ru-GO /NA/ SPGE and Ru-Au /NA/ SPGE were calculated to be 2.03×10^{-4} cm/s and 0.16×10^{-4} cm/s, respectively. Obviously, The K_{et} value of Ru-GO /NA was higher than Ru-Au /NA, indicating a higher rate of electron transfer between redox species and the Ru-GO compared to the Ru-Au modified SPGE interface. This finding confirms that nanocomposites can assist the modified electrode in accelerating electron transfer, whereas Nafion with a negatively charged group (SO_3^-) can help to improve resistance to anions and bulky compounds and allow it to pre-concentrate the target cations. The EIS analysis results are consistent with cyclic voltammogram studies.

Anodic stripping voltammetry was applied to study the performance of developed sensors toward cadmium and lead detection in a solution containing 200 ppb of each metal species in 0.1 M acetate buffer (pH 5.0). The recorded voltammograms are seen in Fig. 3**. b.,** presenting a higher stripping current for the modified hybrid nanocomposites compared to bare SPGE. Obviously, Ru-GO provides excellent electrochemical performance for cadmium detection, suggesting that cadmium cation can be accumulated more on the Ru-GO/NA electrode compared to the Ru-Au surface. In contrast, the lead current is higher at Ru-Au by about 15 % compared to the GO-Ru electrode.

3.2. Optimization studies

3.2.1. Effect of pH and Nafion concentration

The pH of the solution has a significant effect on the electrochemical behavior of the modified $Ru(bpy)_3^{2+}$- GO/NA/ SPGE. Thus, A series of acetic acid buffers with different pH values were examined to determine the optimal pH conditions. Fig. 4**. a** shows the influence of pH on the stripping currents of cadmium and lead with a gradual increase from 4.0 to 5.0, as well as the observation of shifted potential toward more negative values with a maximum current response of 151 μA and 142 μA for cadmium and lead respectively. Beyond pH 5, the current response was reduced considerably, and the potential tended to shift to more positive values, promoting the interferent's interaction. The dependence intensity on the Nafion concentration, which was incorporated into the hybrid nanomaterials, was investigated in the range of 0.1–1.5 %. The analysis findings revealed that the current response gradually increased as Nafion concentration increased **(**Fig. 4**. b)**. Obviously, when 1 % Nafion was applied, the stripping current reached its maximum. The signal then decreased slightly as the concentration kept increasing due to the nature of the Nafion film, which became thicker and prevented the physical diffusion of analytes when the Nafion concentration increased. As a result,1 % Nafion was used in the experimental analysis. Similarly, the effect of Ph and Nafion concentration ware studied at Ru-Au /NA/ SPGE. It was observed that the peak current increased gradually for both analytes, reaching the maximum current response of 80 μA and 250 μA for cadmium and lead, respectively. The current then tends to be reduced rapidly. Thus, pH 5 was selected as the effective condition. Additionally, the amount of Nafion concentration mixed with Ru-Au was also tested. The results revealed that as the concentration of Nafion increased, the current response increased gradually, achieving the maximum at 1 % Nafion. Consequently, 1 % Nafion was selected for experimental studies.

3.2.2. Stripping time, potential, and stirring speed

Square wave anodic stripping voltammetry (SWASV)was conducted to optimize striping time and potential towards the detection of ions using Ru-GO/NA/SPGE in 0.1 M acetate buffer (pH 5.0). The stripping currents improved gradually when the potential increased from −0.9 to −1.5 V. Apparently, at −1.6 V, a massive increase in current was reported, implying that at this potential, a high concentration of analytes is accumulating on the Ru-GO/NA modified SPE (Fig. 5**. a**) Additionally, the accumulation time was varied at 30 s, 60 s, 90 s, 120 s, 240 s, and 300 s and the deposition potential was set constant at −1.6 V. Obviously, as seen in Fig. 5**. b,** the peak currents were constantly and linearly increasing with deposition time, reaching the maximum at 300 s. Taking into account the cost factor, 120 s was selected for further experiments. The influence of stirring speed on the metal stripping current was also examined, and the result is seen in Fig. 5**. c**. Obviously, the peak currents of cadmium and lead increased constantly as the stirring speed increased from 30 to 600 rpm. As the Levich equation states, the stripping current plot demonstrates that mass transport behavior is sequentially proportional to the square root of the electrode stirring speed (Fig. 5**. d)** [45]. SWASV was also conducted to investigate the effect of stripping time, potential, and stirring speed on the metal's detection using Au-Ru/ /NA/ SPGE. The time of 120 s and the potential of −1.6 V were selected for further study (Fig. S2 in supporting materials).

3.3. Calibration, repeatability, and reproducibility

Under the optimum condition, square wave anodic stripping voltammetry (SWASV) was applied for the simultaneous determination of cadmium and lead in 0.1 M acetate buffer (pH 5.0) using $[Ru(bpy)_3]^{2+}$-GO/NA/ SPGE and $[Ru(bpy)_3]^{2+}$- Au/NA/ SPGE. As seen in Fig. 6**. a,** with increasing cadmium and lead concentrations, the stripping peak currents increased, indicating a linear relationship over the range 50–350 ppb with a correlation coefficient of 0.9998 and 0.9996 for cadmium and lead, respectively **(**Fig. 6**.b)**. Based on the slope of the linear curve, the sensitivity of the developed sensor is 0.8 μA/ppb for cadmium and 0.7 μA/ppb for lead. The limit of detection and quantification were calculated for cadmium to be 4.2 ppb and 15.06 ppb, respectively, and for lead, 5.3 ppb and 18.09 ppb. For $[Ru(bpy)_3]^{2+}$- Au/NA/ SPGE, the stripping peak currents increased with increasing lead concentrations over the range 10–300 ppb and cadmium concentrations

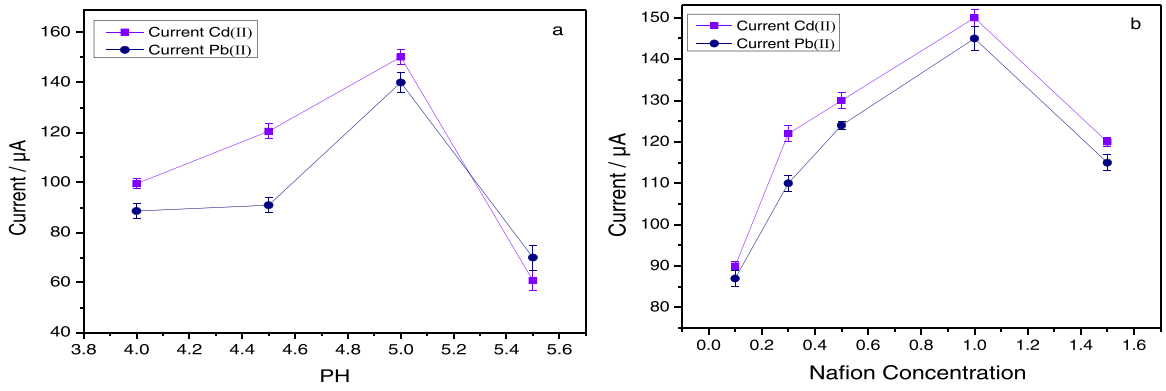

Fig. 4. (a) Effect of pH (a) and Nafion concentration (b) on the stripping current of 200 ppb Cd (II) and Pb (II) in 0.1 M acetate buffer (pH 5.0) at GO-Ru/NA/SPGE.

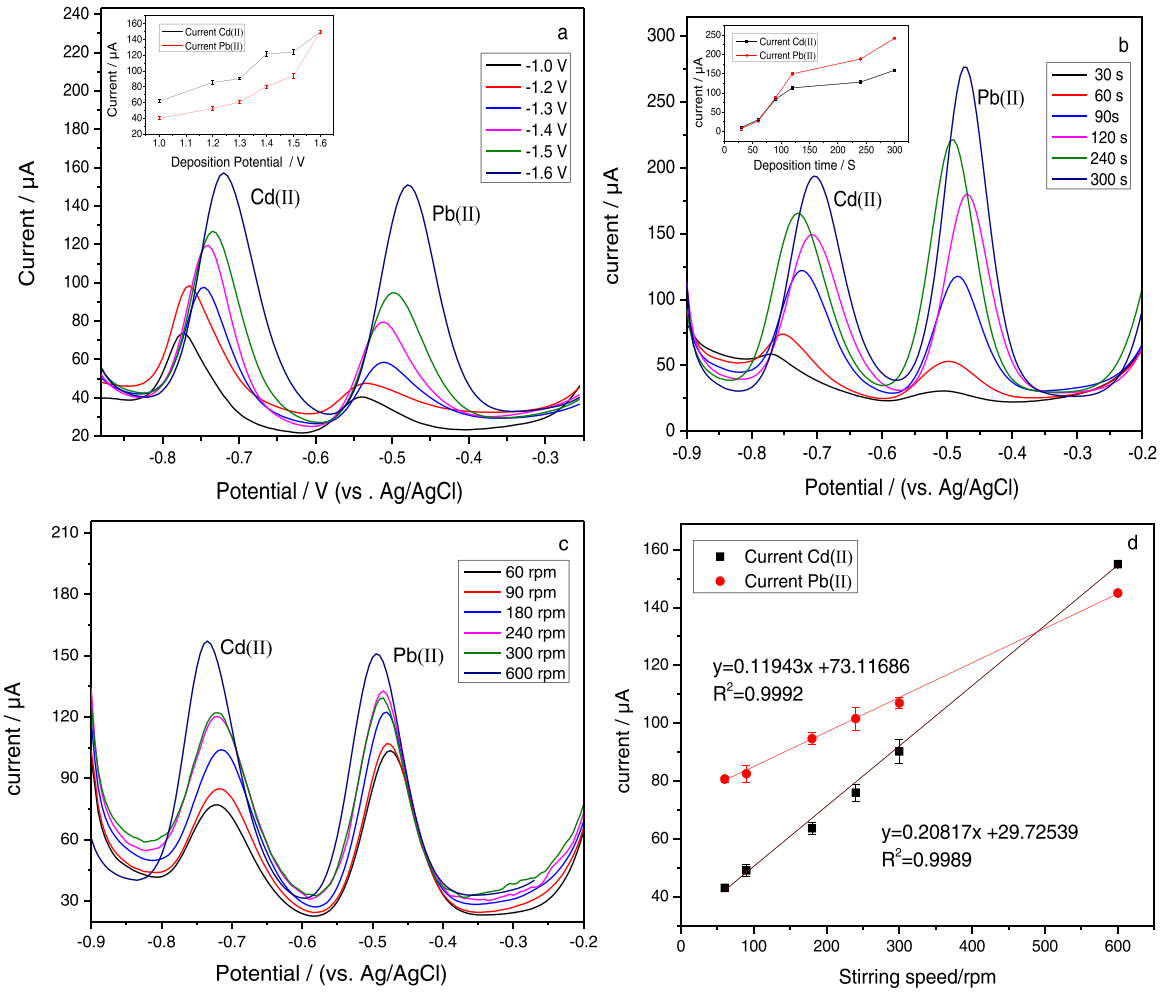

Fig. 5. SWASV of 200 ppb Cd (II) and Pb (II) in 0.1 M acetate buffer (pH 5.0) at GO-Ru/NA/SPGE with a deposition potential ranging from −1.0 V to −1.6 V (a), with a deposition time ranging from 30 to 300 s (b); plot of peak currents vs. deposition potentials (a) (inset), and vs. deposition times (b) (inset). Effect of stirring speed ranging from 60 rpm to 600 rpm (c). Plot of peak currents vs. stirring speed (d).

over the range 100–300 ppb, as shown in Fig. 6**.c, d**, indicating a linear relationship with a correlation coefficient of 0.9992 and 0.09994 for cadmium and lead respectively. Additionally, the limit of detection and quantification were determined for cadmium to be 12.01 ppb and 36.39 ppb and for lead to be 2.5 ppb and 11.8 ppb, with a sensitivity of 0.7 µA/ppb and 1.4 µA/ppb for cadmium and lead, respectively. The repeatability and reproducibility of the hybrid nanocomposite $[Ru(bpy)_3]^{2+}$-GO/NA/ and $[Ru(bpy)_3]^{2+}$- Au/NA/ sensors were examined in the presence of 200 ppb cadmium and lead in 0.1 M acetate buffer (pH 5.0) using SWASV, indicating an excellent degree of reproducibility and repeatability of the present sensors (supporting materials).

3.4. *Effect of interference and stability*

To identify the selectivity of the nanocomposite assays, the 20-fold concentration of ions, including Hg (II), Ni (II), Zn (II), Fe (III), and Cu (II), were examined in the presence of 200 ppb Cd (II) and Pb (II). Fig. 7**.a** shows the stripping response of the assays against interfering ions. Obviously, there was a slight effect toward Pb (II) with a decrease of less than 7 %, indicating a minor change can be recorded compared to the Cd (II) response. The influence of Hg (II) and Zn (II) on Cd (II) stripping current was significant, with a reduction by about 30 %, whereas other interfering ions generated a decrease by 20 %. Possible interference by ionic species in stripping voltammetric detection was also investigated using Ru-Au/NA SPGE. The results are summarized in Fig. 7**.b** There is an increase in the current response of lead by 20 % in the presence of Cu (II) and Hg (II), whereas, in the presence of Ni (II), Zn (II), and Fe (III), there is more than 25 % suppression of the stripping response. The effect of interfering ions on the stripping response of Cd (II) has been studied, and the results showed that the Hg (II), Zn (II), and Cu (II) had an effect by about 20–30 %. Other metals do not have a significant effect on the Cd (II) response. This interference is caused by several factors, such as the formation of intermetallic compounds and the competition for Ru-GO/NA and Ru-Au/NA SPGE active sites between interfering ions and analytes. Additionally, the developed Ru-GO/NA/SPGE and Ru-Au/NA/SPGE were evaluated for long-term stability in the presence of 200 ppb cadmium and lead. As seen in Fig. 7**.c**, after one month, the findings confirm a high current response for Cd (II) and Pb (II) with retained sensitivity of 92 % and 95 %, respectively, promising that the developed sensors had excellent stability. The stability of the Ru-Au/NA assay was also studied, as apparent from Fig. 7**.d**, presenting very good results for both analytes.

3.5. *Real sample analysis*

The developed hybrid Ru-GO/NA and Ru-Au/NA nanocomposite sensors were evaluated to measure the quantity of cadmium and lead in river and tap water samples using SWASV. As presented in Table 1., for both species, the spiked samples' recovery values ranged between 87 % and 103 %. With RSD $\leq$ 7.2 % using Ru-GO/NA and between 88 % and

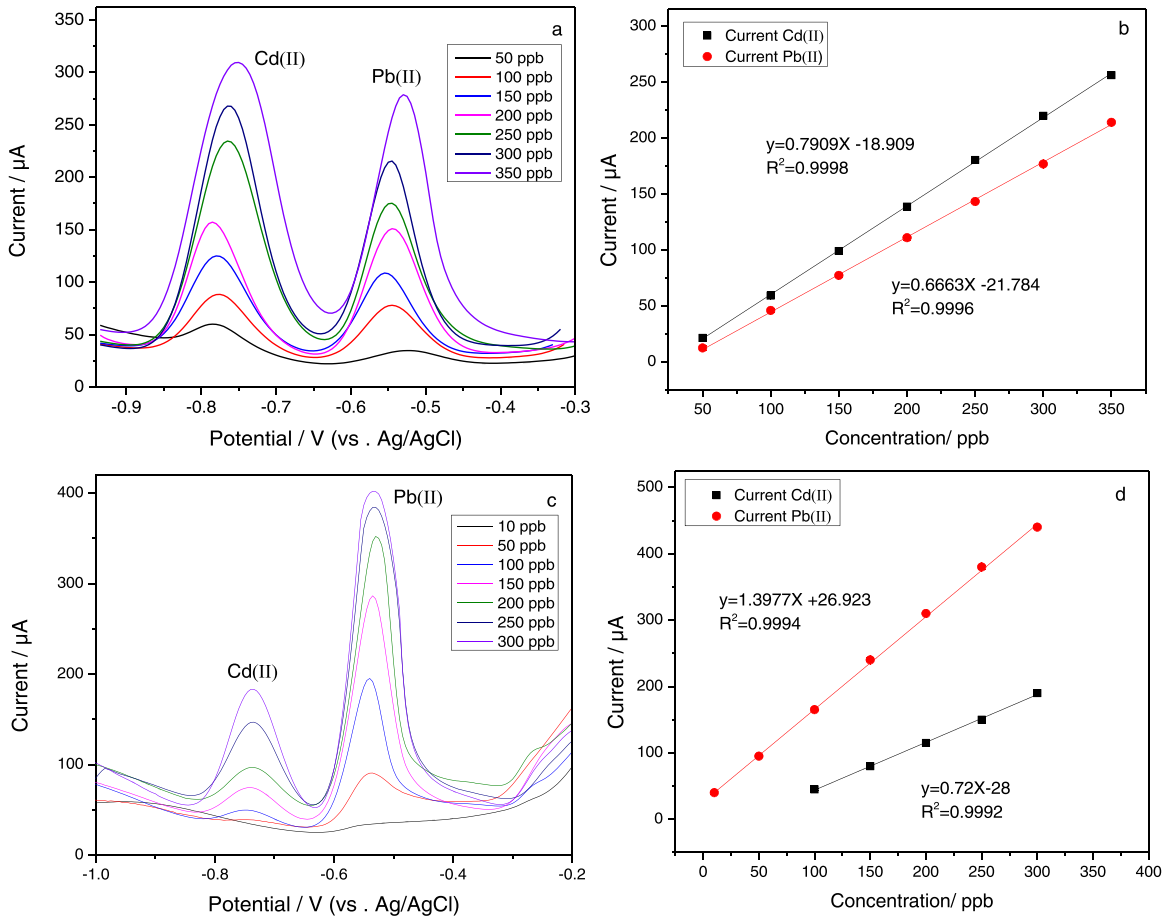

Fig. 6. (a) SWASV of GO-Ru/NA/SPGE with different concentrations of Cd (II) and Pb (II) (50–350ppb). (b) The plot of peak currents of Cd (II) and Pb (II) vs. concentrations for GO-Ru/NA/SPGE. (c) SWASV of Au-Ru/NA/SPGE with different concentrations of Cd and Pb (II) (10–300ppb). (d) The plot of peak currents of Cd (II) and Pb (II) vs. concentrations for Au-Ru/NA/SPGE.

117.3 % with RSD $\leq$ 9.3 % using Ru-Au/NA, assuming that the developed sensors are capable of quantitative determination of both metal ions with very precise results. Moreover, the recovery tests for metallic analytes were determined using AAS as a conventical method, and the values ranged between 88.6 % and 120 %, with RSD $\leq$ 1.6. In comparison, it was observed that the results obtained by present sensors are more sensitive to lead detection than the traditional approach.

4. Conclusion

In the present study, sensitive electrochemical assays based on ruthenium complex were developed for cadmium and lead detection in water samples. The electrostatic interaction between graphene (GO) oxide/citrate-capped gold nanoparticles (AuNPs) and ruthenium (II) bipyridine complex ($[Ru(bpy)_3]^{2+}$) was assessed in the presence of Nafion polymer, and the research revealed that the Nafion has a major contribution to accelerating electron transport and improving electrode stability. The electrocatalytic behavior of $[Ru(bpy)_3]^{2+}$-GO/Nafion and $[Ru(bpy)_3]^{2+}$-Au/Nafion towards the simultaneous detection of metals ion were investigated using anodic stripping square wave voltammetry. Energy dispersive X-ray spectroscopy and scanning electron microscopy were used to assess the surface morphologies of screen-printed electrodes, as well as cyclic voltammetry and electrochemical impedance spectroscopy. The developed hybrid $[Ru(bpy)_3]^{2+}$-Au/Nafion nanocomposite assay shows a good sensitivity towards cadmium ion compared to $[Ru(bpy)_3]^{2+}$-Au/Nafion sensor. The limits of detection were determined to be 4.2 ppb and 5.3 ppb for cadmium and lead, respectively using $[Ru(bpy)_3]^{2+}$-Au/Nafion, and 12.01 ppb and 2.5 ppb using $[Ru(bpy)_3]^{2+}$-Au/Nafion. The disposable sensors were successfully applied in the river and tap water samples, and the recovery values ranged between 87 % and 103 % with RSD $\leq$ 7.2 % using Ru-GO/NA and between 88 % and 117.3 % with RSD $\leq$ 9.3 % using Ru-Au/NA, indicating that the developed sensors have potential to determine the concentration of analyte ions with very precise results.

Funding

The Saudi Ministry of Higher Education supported this work.

CRediT authorship contribution statement

Ibtihaj Albalawi, Conceptualization, Formal analysis, Data curation, Methodology, Investigation, Resources, Software, Validation, Visualization, Funding acquisition, Writing – original draft, Writing – review & editing. **Anna Hogan,** Investigation, Validation, Software **Hanan Alatawi,** Investigation, review & editing, **Samia Alsefri**, Investigation, review & editing. **Eric Moore,** Conceptualization, Project administration, Supervision, Visualization, Funding acquisition, Writing – review & editing.

Declaration of Competing Interest

The authors declare that they have no known competing financial interests or personal relationships that could have appeared to influence the work reported in this paper.

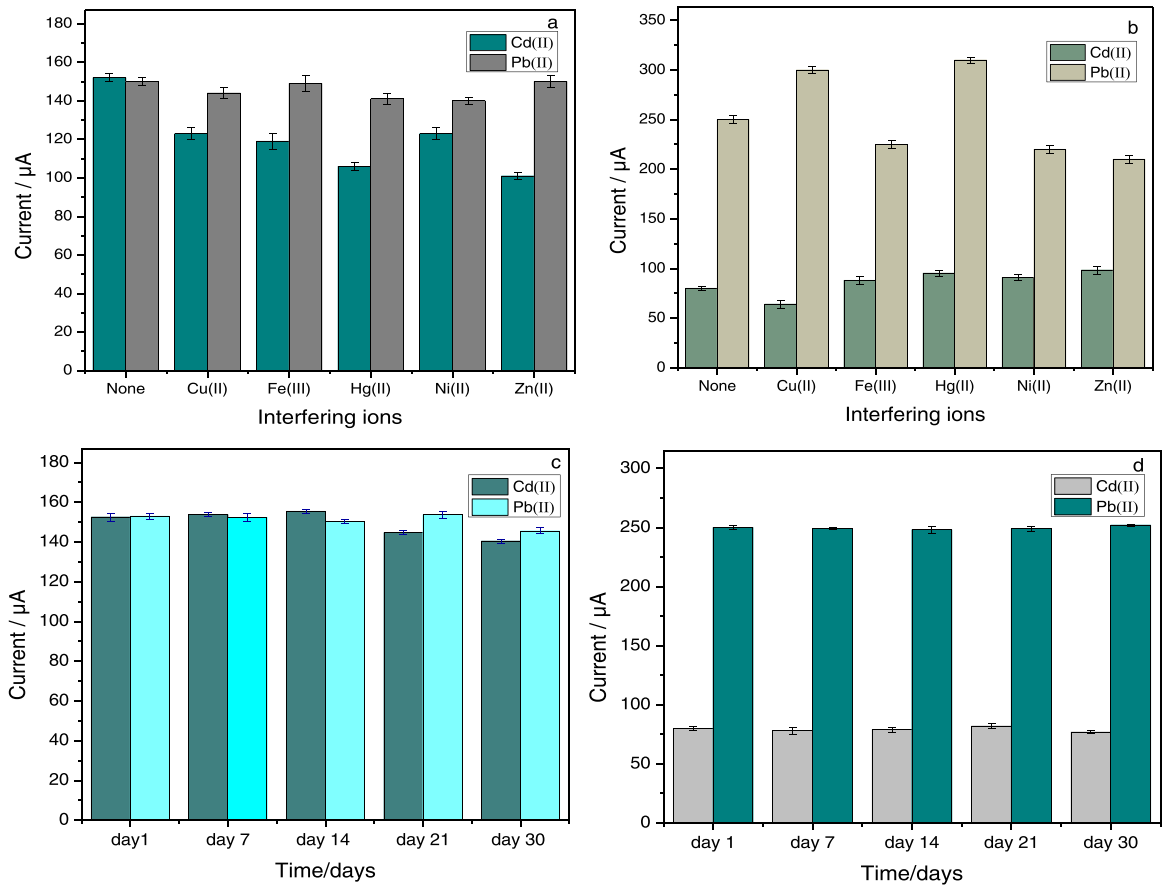

Fig. 7. The effect of interferences using GO-Ru/NA/SPGE (a) and Au-Ru/NA/SPGE (b) on the current of 200 ppb Cd (II) and Pb (II) using 20-fold of each metal separately. The stability of GO-Ru/NA/SPGE (c) and Au-Ru/NA/SPGE (d) in the presence of 200 ppb Cd (II) and Pb (II) in 0.1 M acetate buffer (pH 5.0).

Table 1
Determination of Cd (II) and Pb (II) in real water samples using GO−Ru/NA/SPGE, Au−Ru/NA/SPGE and traditional F-AAS.

Techniques	Sample	Added (ppb)		Found (ppb)		Recovery %		RSD %	
		Cd	Pb	Cd	Pb	Cd	Pb	Cd	Pb
Ru-GO/NA/SPGE	River water	150	150	154.4	130.3	103	86.9	7.2	4.3
	Tap water	150	150	147	135	98	90	5.3	6.7
Ru-Au/NA/SPGE	River water	150	150	176	156	117.3	104	8.2	5.6
	Tap water	150	150	152	132.2	101.3	88	9.3	6.6
F-AAS	River water	150	150	183	133	120	88.6	1.9	1.6
	Tap water	150	150	155	139.5	103.3	93	1.4	1.8

Data availability

Data will be made available on request.

Acknowledgments

The author thanks the Environmental research institution (ERI) and Tyndall institution for providing access to scientific research facilities and labourites.

Appendix A. Supporting information

Supplementary data associated with this article can be found in the online version at doi:10.1016/j.snb.2022.133273.

References

[1] M. Priyadarshanee, S. Das, Biosorption and removal of toxic heavy metals by metal tolerating bacteria for bioremediation of metal contamination: a comprehensive review, J. Environ. Chem. Eng. 9 (2021), 104686, https://doi.org/10.1016/j.jece.2020.104686.

[2] K.B.S. Perelonia, K.C.D. Benitez, R.J.S. Banicod, G.C. Tadifa, F.D. Cambia, U. M. Montojo, Validation of an analytical method for the determination of cadmium, lead and mercury in fish and fishery resources by graphite furnace and cold vapor atomic absorption spectrometry, Food Control 130 (2021), 108363, https://doi.org/10.1016/j.foodcont.2021.108363.

[3] N. Salehi, A. Moghimi, H. Shahbazi, Magnetic nanobiosorbent (MG-Chi/Fe3O4) for dispersive solid-phase extraction of Cu(II), Pb(II), and Cd(II) followed by flame atomic absorption spectrometry determination, IET Nanobiotechnol 15 (2021) 575–584, https://doi.org/10.1049/nbt2.12025.

[4] S. Azimi, Z. Es'haghi, A magnetized nanoparticle based solid-phase extraction procedure followed by inductively coupled plasma atomic emission spectrometry to determine arsenic, lead and cadmium in water, milk, indian rice and red tea, Bull. Environ. Contam. Toxicol. 98 (2017) 830–836, https://doi.org/10.1007/s00128-017-2068-8.

[5] E. Bozorgzadeh, A. Pasdaran, H. Ebrahimi-Najafabadi, Determination of toxic heavy metals in fish samples using dispersive micro solid phase extraction combined with inductively coupled plasma optical emission spectroscopy, Food Chem. 346 (2021), 128916, https://doi.org/10.1016/j.foodchem.2020.128916.

[6] R. Mohamed, B.H. Zainudin, A.S. Yaakob, Method validation and determination of heavy metals in cocoa beans and cocoa products by microwave assisted digestion technique with inductively coupled plasma mass spectrometry, Food Chem. 303 (2020), 125392, https://doi.org/10.1016/j.foodchem.2019.125392.

[7] L. Suo, X. Dong, X. Gao, J. Xu, Z. Huang, J. Ye, X. Lu, L. Zhao, Silica-coated magnetic graphene oxide nanocomposite based magnetic solid phase extraction of trace amounts of heavy metals in water samples prior to determination by inductively coupled plasma mass spectrometry, Microchem. J. 149 (2019), 104039, https://doi.org/10.1016/j.microc.2019.104039.
[8] A. Garciá-Miranda Ferrari, P. Carrington, S.J. Rowley-Neale, C.E. Banks, Recent advances in portable heavy metal electrochemical sensing platforms, Environ. Sci. (Camb.) 6 (2020) 2676–2690, https://doi.org/10.1039/d0ew00407c.
[9] A. Nsabimana, S.A. Kitte, T.H. Fereja, M.I. Halawa, W. Zhang, G. Xu, Recent developments in stripping analysis of trace metals, Curr. Opin. Electrochem. 17 (2019) 65–71, https://doi.org/10.1016/j.coelec.2019.04.012.
[10] C. Arino, C. Banks, A. Bobrowski, R. Crapnell, A. Economou, A. Krolicka, C. Perez-Rafols, D. Soulis, J. wang, Electrochemical stripping analysis, Nat. Rev. Methods Prim. 2 (2022) 62, https://doi.org/10.1038/s43586-022-00143-5.
[11] D.K. Pattadar, J.N. Sharma, B.P. Mainali, F.P. Zamborini, Anodic stripping electrochemical analysis of metal nanoparticles, Curr. Opin. Electrochem. 13 (2019) 147–156, https://doi.org/10.1016/j.coelec.2018.12.006.
[12] A. Jawed, V. Saxena, L.M. Pandey, Engineered nanomaterials and their surface functionalization for the removal of heavy metals: a review, J. Water Process Eng. 33 (2020), 101009, https://doi.org/10.1016/j.jwpe.2019.101009.
[13] Z. Peng, X. Liu, W. Zhang, Z. Zeng, Z. Liu, C. Zhang, Y. Liu, B. Shao, Q. Liang, W. Tang, X. Yuan, Advances in the application, toxicity and degradation of carbon nanomaterials in environment: a review, Environ. Int 134 (2020), https://doi.org/10.1016/j.envint.2019.105298.
[14] L.P. Lingamdinne, J.R. Koduru, R.R. Karri, A comprehensive review of applications of magnetic graphene oxide based nanocomposites for sustainable water purification, J. Environ. Manag. 231 (2019) 622–634, https://doi.org/10.1016/j.jenvman.2018.10.063.
[15] A.I.A. Sherlala, A.A.A. Raman, M.M. Bello, A. Asghar, A review of the applications of organo-functionalized magnetic graphene oxide nanocomposites for heavy metal adsorption, Chemosphere 193 (2018) 1004–1017, https://doi.org/10.1016/j.chemosphere.2017.11.093.
[16] F. Chi-Ming Leung, V.Wing-Wah Yam, Covalent and non-covalent conjugation of few-layered graphene oxide and ruthenium(II) complex hybrids and their energy transfer modulation via enzymatic hydrolysis, ACS Appl. Mater. Interfaces 10 (2018) 15582–15590, https://doi.org/10.1021/acsami.7b18663.
[17] T.T. Meng, Z.B. Zheng, K.Z. Wang, Layer-by-layer assembly of graphene oxide and a Ru(II) complex and significant photocurrent generation properties, Langmuir 29 (2013) 14314–14320, https://doi.org/10.1021/la403428q.
[18] K. Loza, M. Heggen, M. Epple, Synthesis, structure, properties, and applications of bimetallic nanoparticles of noble metals, Adv. Funct. Mater. 30 (2020), https://doi.org/10.1002/adfm.201909260.
[19] N. Sarfraz, I. Khan, Plasmonic gold nanoparticles (AuNPs): properties, synthesis and their advanced energy, environmental and biomedical applications, Chem. Asian J. 16 (2021) 720–742, https://doi.org/10.1002/asia.202001202.
[20] T. Khan, N. Ullah, M.A. Khan, Z. ur R. Mashwani, A. Nadhman, Plant-based gold nanoparticles; a comprehensive review of the decade-long research on synthesis, mechanistic aspects and diverse applications, Adv. Colloid Interface Sci. 272 (2019), 102017, https://doi.org/10.1016/j.cis.2019.102017.
[21] H.N. Verma, P. Singh, R.M. Chavan, Gold nanoparticle: synthesis and characterization, Vet. World 7 (2014) 72–77, https://doi.org/10.14202/vetworld.2014.72-77.
[22] C. Daruich De Souza, B. Ribeiro Nogueira, M.E.C.M. Rostelato, Review of the methodologies used in the synthesis gold nanoparticles by chemical reduction, J. Alloy. Compd. 798 (2019) 714–740, https://doi.org/10.1016/j.jallcom.2019.05.153.
[23] J. Turkevich, P.C. Stevenson, J. Hillier, A study of the nucleation and growth processes in the synthesis of colloidal gold, Discuss. Faraday Soc. 11 (1951) 55–75, https://doi.org/10.1039/DF9511100055.
[24] C. Daruich De Souza, B. Ribeiro Nogueira, M.E.C.M. Rostelato, Review of the methodologies used in the synthesis gold nanoparticles by chemical reduction, J. Alloy. Compd. 798 (2019) 714–740, https://doi.org/10.1016/j.jallcom.2019.05.153.
[25] F. Dumur, E. Dumas, C.R. Mayer, Functionalization of gold nanoparticles by inorganic entities, Nanomaterials 10 (2020), https://doi.org/10.3390/nano10030548.
[26] P. Perez-Tejeda, E. Grueso, A. Marin-Gordillo, C. Torres-Marquez, R.M. Giráldez-Pérez, Aqueous gold nanoparticle solutions for improved efficiency in electrogenerated chemiluminescent reactions, ACS Appl. Nano Mater. 1 (2018) 5307–5315, https://doi.org/10.1021/acsanm.8b01323.
[27] G.G. Gagliardi, A. Ibrahim, D. Borello, A. El-Kharouf, Composite polymers development and application for polymer electrolyte membrane technologies-a review, Molecules 25 (2020), https://doi.org/10.3390/molecules25071712.
[28] Y. Qu, X. Liu, X. Zheng, Z. Guo, Preparation of Nafion-Ru(bpy)3 2+-chitosan/gold nanoparticles composite film and its electrochemiluminescence application, Anal. Sci. 28 (2012) 571–576, https://doi.org/10.2116/analsci.28.571.
[29] M. Hosseini, M.R.K. Pur, P. Norouzi, M.R. Moghaddam, M.R. Ganjali, An enhanced electrochemiluminescence sensor modified with a Ru(bpy)32 +/Yb2O3 nanoparticle/nafion composite for the analysis of methadone samples, Mater. Sci. Eng. C. 76 (2017) 483–489, https://doi.org/10.1016/j.msec.2017.03.070.
[30] L. Li, L. Zhou, X. Liu, T. You, Ultrasensitive self-enhanced electrochemiluminescence sensor based on novel PAN@Ru@PEI@Nafion nanofiber mat, J. Mater. Chem. B 8 (2020) 3590–3597, https://doi.org/10.1039/c9tb02287b.
[31] D. Bahari, B. Babamiri, A. Salimi, R. Hallaj, S.M. Amininasab, A self-enhanced ECL-RET immunosensor for the detection of CA19-9 antigen based on Ru(bpy)2(phen-NH2)2+ - Amine-rich nitrogen-doped carbon nanodots as probe and graphene oxide grafted hyperbranched aromatic polyamide as platform, Anal. Chim. Acta 1132 (2020) 55–65, https://doi.org/10.1016/j.aca.2020.07.023.
[32] X. Xiong, Y. Zhang, Y.F. Wang, H.F. Sha, N. Jia, One-step electrochemiluminescence immunoassay for breast cancer biomarker CA 15-3 based on Ru(bpy)62+-coated UiO-66-NH2 metal-organic framework, Sens Actuators B Chem. 297 (2019), 126812, https://doi.org/10.1016/j.snb.2019.126812.
[33] X. Xiong, P. Zhang, Y. Lu, S. He, Y. Zhang, N. Jia, A dual-signal electrochemiluminescence immunosensor based on Ru(bpy)32+@3D-foam graphene and SnS2 dots for sensitive detection of gastric cancer biomarker CA 72-4, Talanta 221 (2021), 121644, https://doi.org/10.1016/j.talanta.2020.121644.
[34] T.B.G. Lopez, S.T. Palisoc, M.T. Natividad, Highly sensitive [Ru(bpy)3]2 +/Nafion® modified indium tin oxide-based sensor for heavy metal detection, Sens. Biosensing Res. 15 (2017) 34–40, https://doi.org/10.1016/j.sbsr.2017.07.001.
[35] M.B. Gumpu, M. Veerapandian, U.M. Krishnan, J.B.B. Rayappan, Simultaneous electrochemical detection of Cd(II), Pb(II), As(III) and Hg(II) ions using ruthenium (II)-textured graphene oxide nanocomposite, Talanta 162 (2017) 574–582, https://doi.org/10.1016/j.talanta.2016.10.076.
[36] X. Sun, Y. Du, S. Dong, E. Wang, Method for effective immobilization of Ru(bpy)32 + on an electrode surface for solid-state electrochemiluminescene detection, Anal. Chem. 77 (2005) 8166–8169, https://doi.org/10.1021/ac051476.
[37] I. Albalawi, A. Hogan, H. Alatawi, E. Moore, A sensitive electrochemical analysis for cadmium and lead based on Nafion-Bismuth film in a water sample, Sens. Biosensing Res. (2021), 100454, https://doi.org/10.1016/j.sbsr.2021.100454.
[38] H. Li, F. Liu, S. Sun, J. Wang, Z. Li, D. Mu, B. Qiao, X. Peng, Interaction of Ru(phen) 3Cl2 with graphene oxide and its application for DNA detection both in vitro and in vivo, J. Mater. Chem. B 1 (2013) 4146–4151, https://doi.org/10.1039/c3tb20858c.
[39] M.B. Gumpu, M. Veerapandian, U.M. Krishnan, J.B.B. Rayappan, Electrochemical sensing platform for the determination of arsenite and arsenate using electroactive nanocomposite electrode, Chem. Eng. J. 351 (2018) 319–327, https://doi.org/10.1016/j.cej.2018.06.097.
[40] K.M. de Oliveira, T.C.C. dos Santos, L.R. Dinelli, J.Z. Marinho, R.C. Lima, A. L. Bogado, Aggregates of gold nanoparticles with complexes containing ruthenium as modifiers in carbon paste electrodes, Polyhedron 50 (2013) 410–417, https://doi.org/10.1016/j.poly.2012.11.014.
[41] X. Wang, W. Liu, C. Li, C. Chu, S. Wang, M. Yan, J. Yu, J. Huang, Synthesis of polyaniline using electrochemical polymerization and application in a sensitive DNA biosensor with [Ru(bpy)3]2+ functionalized nanoporous gold composite as label, Mon. Chem. 144 (2013) 1759–1765, https://doi.org/10.1007/s00706-013-1073-9.
[42] P. Zhang, J. Wang, H. Huang, B. Yu, K. Qiu, J. Huang, S. Wang, L. Jiang, G. Gasser, L. Ji, H. Chao, Unexpected high photothemal conversion efficiency of gold nanospheres upon grafting with two-photon luminescent ruthenium(II) complexes: a way towards cancer therapy, Biomaterials 63 (2015) 102–114, https://doi.org/10.1016/j.biomaterials.2015.06.012.
[43] X. Huang, Y. Li, X. Zhang, X. Zhang, Y. Chen, W. Gao, An efficient signal-on aptamer-based biosensor for adenosine triphosphate detection using graphene oxide both as an electrochemical and electrochemiluminescence signal indicator, Analyst 140 (2015) 6015–6024, https://doi.org/10.1039/c5an00769k.
[44] A.G.M. Ferrari, C.W. Foster, P.J. Kelly, D.A.C. Brownson, C.E. Banks, Determination of the electrochemical area of screen-printed electrochemical sensing platforms, Biosensors (Basel) 8 (2018), https://doi.org/10.3390/bios8020053.
[45] S.K. Pandey, S. Sachan, S.K. Singh, Ultra-trace sensing of cadmium and lead by square wave anodic stripping voltammetry using ionic liquid modified graphene oxide, Mater. Sci. Energy Technol. 2 (2019) 667–675, https://doi.org/10.1016/j.mset.2019.09.004.

Ibtihaj Albalawi Has obtained BSc (Hons) degree in chemistry from the University of Tabuk in Saudi Arabia and MSc degree in analytical chemistry (Environmental analysis) from University College Cork. Currently, she is doing her Ph.D. in electrochemical sensing technology.

Anna Hogan has been in the teaching and research profession for almost 20 years. She is working in the area of separation science.

Hanan Alatawi has a degree of Master of Science in analytical chemistry. She is currently studying Ph.D. in Analytical chemistry. Her research interests are in separation science and microfluidic capillary electrophoresis system.

Samia Alsefri is studying as a doctor in the School of Chemistry, University College of Cork, Ireland. Her research interests include electrochemical biosensors and electrochemical sensors.

Dr. Eric Moore is a Senior Lecturer in the School of Chemistry and heads a research group at University College Cork focused on chemical and bio-sensing and separation. He is an Academic member within the Life Science Interface group at Tyndall National Institute, University College Cork. Since 2010 he has led an active research team with very strong industry engagement, which is a critical part of his research strategy. He has extensive linkages with the pharmaceutical, biopharmaceutical, biomedical device, environment and food/beverage sectors. He has championed postgraduate education, especially at the MSc level and is dedicated to providing high calibre industry ready graduates.